TOPOGRAPHIC MAPPING OF MARS: FROM HECTOMETER TO MICROMETER SCALES

R. L. Kirk[1*], S. W. Squyres[2], G. Neukum[3], and the MER Athena and MEX HRSC Science Teams

[1]U.S. Geological Survey, 2255 N. Gemini Dr., Flagstaff, Arizona 86001 USA – rkirk@usgs.gov
[2]Cornell University Dept. of Astronomy, Ithaca, New York, USA – squyres@astro.cornell.edu
[3]Freie Universität, Institute for Geosciences, Berlin, Germany – gneukum@zedat.fu-berlin.de

Commission IV, WG IV/9

KEY WORDS: Extraterrestrial, planetary, Mars, topography, photogrammetry, cartography, remote sensing, exploration

ABSTRACT:

We describe USGS topomapping of Mars at resolutions from 100 m to 30 μm with data from the latest spacecraft missions. Analysis of NASA 2001 Mars Odyssey Thermal Emission Imaging System (THEMIS) data combining daytime visible reflected, daytime IR emitted, and nighttime IR emitted images allows us to isolate the physical effects of topography, albedo, and thermal inertia. To a good approximation these physical influences interact linearly so that maps showing topographic shading, albedo, and relative thermal inertia can be produced by simple algebraic manipulation of the coregistered images. The shading map resembles an airbrush shaded relief portrayal of the surface, and can be used as the input for quantitative reconstruction of topography by photoclinometry (PC) at 100-m resolution over most of the planet.
The High Resolution Stereo Camera (HRSC) of the ESA Mars Express orbiter includes a 9-line scanner for color and stereo imaging and a Super-Resolution Channel (SRC). We analyze these images with a combination of USGS ISIS cartographic software and commercial photogrammetric software, providing an independent check on the stereo processing pipeline developed by the HRSC team. In particular, we are producing very high resolution digital elevation models (DEMs) from the SRC images by photoclinometry and by stereoanalysis, using Mars Orbiter Camera images to complete the stereopair.
The NASA Mars Exploration Rovers (MER) carry a diverse set of cameras: two wide-angle hazard camera pairs, panoramic stereo imagers (Pancam and Navcam), and a Microscopic Imager (MI) that images a 3-cm-square area at 30 μm/pixel resolution. Our work emphasizes MI data and includes geometric calibration, bundle-adjustment, mosaicking, generation of DEMs by stereoanalysis and focal sectioning, and combination of MI images with color data from Pancam. The software being developed to support these analyses can also be used to produce high-precision controlled mosaics, DEMs, and other products from the Pancam and Navcam images.

1. INTRODUCTION

The four spacecraft sent from Earth to Mars during the 2001 and 2003 opportunities each carry novel imagers that open up new possibilities for topographic mapping of Mars. In this paper we describe the techniques that we are developing at the U.S. Geological Survey in order to exploit these datasets and show examples of the results. A noteworthy aspect of the work described here is the enormous range in spatial scales at which mapping is possible. The THEMIS imagery is relatively low resolution and nonstereo but we have developed a novel processing technique that effectively "strips away" the albedo variations that normally limit photoclinometry (or "shape-from-shading") techniques to small areas of more uniform properties. The dataset and method make topographic mapping of most or all of the planet at hectometer resolution possible for the first time. The HRSC multiline stereo scanner is the first instrument of its kind to be used in planetary exploration, and is returning color and robust, single-pass stereo imagery of large areas of Mars at decameter resolutions. We have developed an independent processing capability for these images, but our efforts are currently focused on our unique capabilities within the HRSC team for topographic mapping with images from the SRC at resolutions of a few meters. The MER rovers achieve higher resolution yet from their positions on the surface of Mars. In particular, the Microscopic Imager is also the first instrument of its kind on Mars and has an unprecedented 30 μm resolution. The other cameras on the rovers bridge the gap between this scale and what can be seen from orbit. The software and procedures we are developing for MER allow us to work flexibly with images from all of the onboard cameras, individually or in combination.

2. 2001 MARS ODYSSEY ORBITER THEMIS

2.1 Source Data

The NASA 2001 Mars Odyssey Orbiter began its mapping mission in February 2002. The THEMIS instrument on Odyssey acquires images (Christensen et al., 2003) in both visible and thermal infrared wavelengths. Visible-light (VIS) images can be acquired in five spectral bands (0.43-0.86 μm) although a single image in Band 3 (a red band ~0.65 μm) is usually collected. This band is ideal for our work because it shows surface albedo variations with high contrast and signal/noise ratio. VIS image strips are ~18 km wide with resolution of ~18 m/pixel. The IR images are of lower resolution (~100 m/pixel), cover a wider swath (~32 km), and can be acquired in 9 bands between 6.8–14.9 μm. For the work described here we use only Band 9 (~12.6 μm), which is always acquired and which has the highest signal/noise for targets at or below 230 K. The VIS images and daytime IR images that we use were acquired simultaneously; those collected at equatorial latitudes have solar incidence angles between ~45° and ~75° (between ~15 h and 16:30 h local time). The nighttime IR images are acquired on the opposite part of the orbit (i.e. between ~3 h and 4:30 h).

2.2 Physical Basis of the Method

A necessary condition for analysis described here is the match between the number of available THEMIS datasets (VIS, day IR, and night IR) and the number of dominant physical influences on these observables: surface orientation, albedo, and thermophysical properties in the guise of thermal inertia (Elachi, 1987). Thermal inertia (I, units are J m^{-2} $sec^{-1/2}$ K^{-1}) is equal to $\sqrt{(k\rho c_p)}$, where k is the

* Corresponding author.

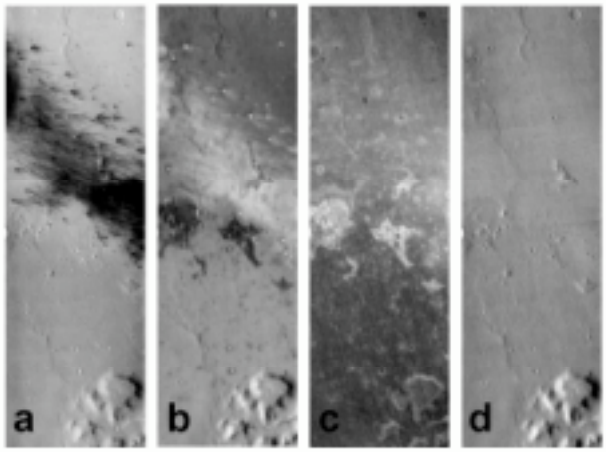

Figure 1. Extraction of topographic radiance image accounting for variations both in relative albedo and thermal inertia. a. Image V0881003RDR.QUB (Band 3), b. Image I0881002RDR.QUB (Band 9). c. Nighttime Image I01511006RDR.QUB (Band 9). d. "Magic airbrush" weighted sum of a, b, c chosen to cancel variations of albedo and thermal inertia. Images cover part of Gusev crater, with the MER-A Spirit landing point to the left of the triangle of hills in the top center.

thermal conductivity, ρ is the density and c_p is the specific heat. For Mars, I ranges from ~50 for very fine dust, to ~300 for fine sand, to ~2000 for solid dense rock (cf. Jakosky and Mellon, 2001; Mellon et al., 2000). A further condition for the success of our analysis is that the influence of these parameters on the observables is sufficiently distinct that they can be disentangled. The VIS image, formed by reflected sunlight, is sensitive to slope orientation as described by the surface photometric function and is proportional to albedo A, but is not affected by thermal properties. The day IR image is formed by energy that has been absorbed and reradiated. For small I this reradiation is mostly instantaneous, and the day image has a Lambertian orientation dependence and is proportional to $(1-A)$; the former is similar to the VIS image but the latter is of the opposite sense. For finite I, the daytime temperature is reduced by thermal conduction to the subsurface and retains a "fading memory" of the past history of insolation. Increasing I has the opposite effect on night temperatures, raising them by conduction from below. Albedo and orientation have weaker influences on the night temperature through the total energy absorbed during the day. From this description it is evident that the THEMIS observations have distinct responses to orientation, A, and I, so that an inversion for these parameters is likely to be robust.

2.3 A "Magic Airbrush"

Mathematically, it is a given that the full thermal model can be linearized for small departures of orientation, albedo, and thermal inertia from some mean values, but will such a linear approximation be valid over a useful parameter space? Theoretical considerations, preliminary investigations with the numerical thermal code "KRC" (Kieffer et al., 1977), and empirical results with THEMIS data suggest the answer is yes. Work now underway with the KRC code will guide us to a strategy for inverting the THEMIS data in the general (nonlinear) case, provide error estimates for the recovered parameters, and lead to an empirical "photometric function" that describes how day IR radiance depends on east-west and north-south slopes.

If p_V represents the visible-band photometric function of the surface and p_{IR} an effective photometric function for the infrared emission, then the accuracy with which albedo variations can be cancelled in a linear combination of the visible image Ap_V and the IR image $(1-A)p_{IR}$ depends on the degree of resemblance between p_V and p_{IR}. As described above, p_{IR} will be nearly Lambertian for small I, whereas p_V for the martian surface at the phase angles of interest is slightly less limb-darkened (Kirk et al., 2000b) and will have only 70–80% the contrast of a Lambertian function. In practice, we find that it is straightforward to determine an empirical combination of the images that cancels both albedo and thermal inertia variations and leaves only slope-related effects as shown in Figure 1. The existence of such a solution depends on the properties of the thermal model as described above; the ease with which it is found is a result of the extreme acuity with which the visual system can distinguish intrinsic effects like albedo (which can affect arbitrarily large patches of the surface in a similar way) from topographic shading (in which dark and bright slopes are typically paired within a small region). We use the informal term "magic airbrush" for the empirical processing of THEMIS images, because it leads to a product (Fig. 1d) that resembles a shaded relief map yet is the result of surprisingly simple image processing rather than the painstaking efforts of an airbrush illustrator.

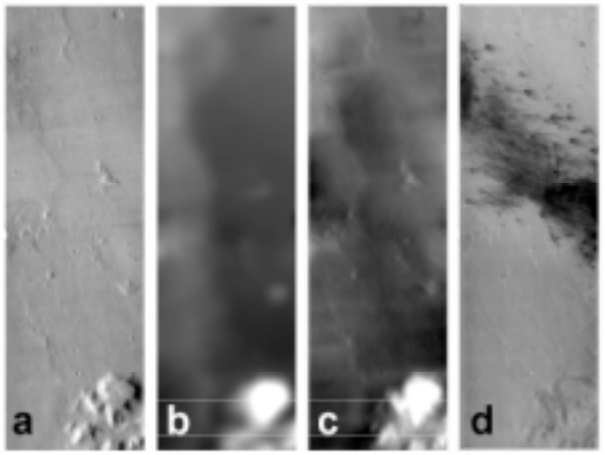

Figure 2. MOLA-controlled photoclinometry to derive high resolution DEM: a. "magic airbrush" as in Fig. 1d, b. MOLA gridded topography, c. THEMIS-based photoclinometry modeled DEM, d. model of relative albedo derived by simulating the VIS image with the DEM and dividing out topographic modulation.

A further requisite for the production of "magic airbrush" maps that requires mention is the accurate coregistration of the component images. The VIS and IR images (Fig. 1a–c) were aligned by resampling them to a common map projection at a sample spacing of 80 m/pixel (a compromise between the VIS and IR resolutions) and then interactively adjusting the position of each dataset to register it to the others and to a control base prepared from Mars Orbiter Laser Altimeter (MOLA) gridded radius data (Smith et al., 2001). We are currently developing tools for correcting the positional errors in THEMIS data by rigorous least-squares bundle adjustment (Archinal et al., 2004).

2.4 Quantitative Topography

The use of the "magic airbrush" images is not limited to qualitative photointerpretation of the morphologic features that they reveal by suppressing albedo variations. The product can also be subjected to analysis by two-dimensional photoclinometry (Kirk, 1987; Kirk et al., 2003b; http://astrogeology.usgs.gov/Teams/Geomatics/pc.html) to produce a DEM with single-pixel resolution. Because of the use of thermal infrared data, this may also be referred to as "thermoclinometry," or "shape-from-heating." A weighted combination of p_V and p_{IR} should properly be used to interpret the weighted sum of VIS and IR images. Until the form of p_{IR} is determined, we empirically resort to a Lambertian function and adjust the contrast of the input image to produce a DEM in which the heights of selected features agree with an independent (but generally lower resolution) source of topographic data such as MOLA (Smith et al., 2001). Such "calibration" of the photoclinometric

process would be required even if the photometric function were precisely known (e.g., even for visible band images without "magic airbrush" processing; see section 3 below and Kirk et al., 2003b) because the image contains a uniform additive offset that affects its constant. This offset comes in part from atmospheric haze in the VIS image, which varies with time and is not known a priori. Figure 2 shows the photoclinometric DEM from the example of Fig. 1, with a MOLA DEM of the same area for comparison. The photoclinometry adds local details while preserving long-wavelength topography such as the height of the 10-km wide mesa at the bottom. The detailed DEM can be used to simulate the VIS image with realistic photometric function p_v but no albedo variations. Dividing the VIS image (after subtraction of a constant haze value) by the simulation yields a map of albedo variations that can reveal subtle features, e.g., the dark slopes on the sides of the mesa in Fig. 2d. The DEM can also be used to map absolute and directional slopes.

We extended the analysis shown in Figs. 1–2 to neighboring THEMIS VIS/IR triplets in order to produce topographic, slope, and albedo maps of essentially the entire MER-A (Spirit) landing ellipse, and also the MER-B (Opportunity) ellipse. These landing sites are among the first areas on Mars for which nearly complete VIS coverage is available, but current mission plans will lead to the eventual collection of global IR imagery and VIS images of about half the planet. MOLA-resolved features that could be used to calibrate photoclinometry were present in only a few of the images, so the remainder were calibrated to have similar slopes on small-scale features. As it happened, Spirit landed within the images shown here, about 2 km west of the triangle of hills seen at the top center. Our THEMIS maps were useful in the early days of the mission for locating the landing point to ~100-m accuracy by tracing sightlines to features visible from the lander. Hypothetical lander locations were also tested by using the DEM to simulate the appearance of the visible horizon. The high resolution of our maps (compared, e.g., to MOLA) was critical for this application.

3. MARS EXPRESS HRSC

3.1 Source Data

In early January 2004, the ESA Mars Express mission started its science phase in orbit around Mars. Imaging and mapping the Martian surface by the High Resolution Stereo Camera (HRSC) is one of the main goals of Mars Express. The HRSC experiment (Albertz et al., 1992; Neukum et al., 2004) is a pushbroom scanning instrument with 9 CCD line detectors mounted in parallel on the focal plane. Its unique feature is the ability to nearly simultaneously obtain imaging data of a specific site at high resolution, with along-track triple stereo, with four colors, and at five different phase angles, thus avoiding any time-dependent variations of the observation conditions. An additional Super-Resolution Channel (HRSC-SRC, a framing device) is yielding nested-in images in the meter-range thus serving as the sharpening eye for detailed photogeologic studies. The spatial resolution from the nominal periapsis altitude of 250 km is 10 m/pixel for the HRSC proper and 2.3 m/pixel for the SRC. The SRC images are normally acquired vertically, but a subset are oblique because of spacecraft maneuvers to fill gaps in image coverage.

3.2 Stereo Mapping Methodology

Our approach to processing HRSC data is largely independent of those used by other members of the camera team, which are described in several papers in this volume (Hauber et al., 2004; Oberst et al., 2004; Ebner et al., 2004; Heipke et al., 2004; Dorrer et al., 2004). We start with images in VICAR format that have been radiometrically calibrated at the German Aerospace Center (DLR) in Berlin. These images are ingested into the USGS in-house digital cartographic software ISIS (Eliason, 1997; Gaddis et al., 1997; Torson and Becker, 1997; see also http://isis.astrogeology.usgs.gov). In particular, the supporting cartographic information in the VICAR labels is converted into its ISIS equivalents. Because ISIS, unlike VICAR, does not currently accommodate changing line exposure times within a scanner image, the images are if necessary broken into multiple files that each have a constant exposure time.

From this point onward, our approach to topographic mapping with the HRSC images is similar to those we have used for a wide range of planetary datasets (Kirk et al., 2000a), and, in particular, for the Mars Global Surveyor MOC images as described in detail in a recent paper (Kirk et al., 2003a). We use ISIS for mission-specific steps (data ingestion and, for most instruments, calibration, though for HRSC the latter has been performed in VICAR), as well as "2D" processing such as map-projection and image mosaicking. The ISIS projection capability now includes orthorectification, and detailed photometric models of the surface and atmosphere (Kirk et al., 2000b, 2001) can be used to correct the images for variations in illumination and atmospheric haze before mosaicking. Two dimensional photoclinometry is also implemented in ISIS (Kirk et al., 2003b).

Our commercial digital photogrammetric workstation running BAE Systems SOCET SET ® software (Miller and Walker, 1993; 1995) is used for "3D" processing steps such as control of the images and automatic extraction and manual editing of DEMs. SOCET SET includes a pushbroom scanner sensor model that is physically realistic but "generic" enough to describe the individual HRSC scanner lines, as well as most images from the Mars Global Surveyor Mars Orbiter Camera (MOC). SRC images can be imported and used with the frame sensor model. We have written software to import these and other types of images from ISIS into SOCET SET and to translate the orientation data in ISIS into the necessary format. In this process, each HRSC detector array must be treated as separate single-line camera, oriented at an appropriate pitch angle to model the true geometry of the instrument. Because SOCET SET is unaware that the images from the different HRSC lines are collected at the same time, the intrinsic robustness of the multiline stereo system is unfortunately lost. This is a relatively minor disadvantage, given the availability of the MOLA global topographic dataset, which provides control with an accuracy on the order of 10 m vertically and 100 m horizontally (Smith et al., 2001; Neumann et al., 2001). The disadvantage is more than made up for in practice by the ability of SOCET SET to perform bundle adjustments that include images from sensors of different types (e.g., SRC and MOC), and to produce DEMs from stereopairs of mixed type. Nevertheless, we plan to extend the bundle-adjustment software being developed for the THEMIS IR scanner (Archinal et al., 2004) to model the HRSC with proper accounting for the constraints between image lines. This software may also eventually be extended to model the high-frequency pointing variations ("jitter") that affect many MOC narrow-angle (NA) images. Because the SOCET SET adjustment software we are now using includes only smoothly varying pointing corrections, we must use ad hoc processing by spatial filtering to remove the jitter-related artifacts from MOC DEMs.

The MOC NA images are well suited in terms of resolution for stereomapping in conjunction with SRC images. The fundamental resolution of the camera is 1.4 m/pixel, but images are most often obtained by pixel summation at resolutions close to 3 or 6 m (Malin and Edgett, 2001). More than 50,000 NA images have been obtained so far (see http://www.msss.com/mars_images/index.html and http://ida.wr.usgs.gov/), and we have been able to locate vertical or near-vertical images that overlap several of the handful of oblique SRC image sets that have been obtained while the Mars Express spacecraft is rolled off of its normal vertical orientation. A larger number of pairs combining off-vertical MOC images with the hundreds of vertical SRC images are

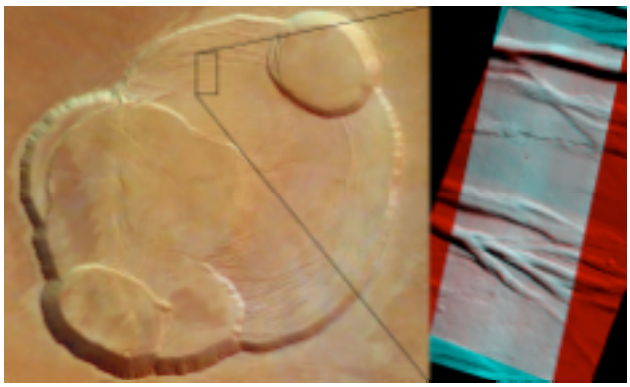

Figure 3. Example of a high-resolution stereopair formed by Mars Global Surveyor MOC and Mars Express HRSC-SRC images. Left, an HRSC color image of the caldera of Olympus Mons showing context. Right, anaglyph combining three 4-m/pixel SRC frames (h0037_0002 through 0004) in red with a 6-m/pixel MOC image (E10-03979) in blue-green. Area of anaglyph is approximately 5x9 km in size and has been rotated slightly to facilitate stereo viewing.

likely to exist. Figure 3 shows an example of a stereopair of part of the caldera of Olympus Mons, consisting of a 6-m/pixel MOC image and a set of three overlapping 4-m/pixel SRC frames. The anaglyph was prepared by projecting the two image sets in ISIS. Figure 4 shows an orthomosaic and contour map derived from a 15 m/post DEM produced from these images in SOCET SET.

3.3 Photoclinometry

Photoclinometry provides another means of producing DEMs with horizontal resolutions of a few meters from SRC images, and one that will be more widely applicable because no high resolution stereo partner is needed. As mentioned previously, photoclinometry must be "calibrated" by determining how much atmospheric haze has reduced the contrast of each image, if quantitatively accurate results are to be obtained for Mars. An independent estimate of the topography is required but can be of lower resolution. Calibration can then be accomplished either by performing trial photoclinometry and adjusting the amount of atmospheric haze subtracted from the image until feature heights agree with the a priori data, or by simulating an image from an a priori DEM and comparing its contrast with the real image (Kirk et al., 2003b). The accuracy of calibration depends on the possibility of finding adequately resolved common features in the image and the topographic dataset. If the only available topography comes from MOLA (which has an effective horizontal resolution of hundreds of meters at best), finding such features can be difficult or impossible, but if a stereo DEM closer to the resolution of the image is available, the photoclinometric topography can be calibrated to 10–20% accuracy in amplitude (Kirk et al., 2003a). Because HRSC stereo images are obtained simultaneously with every SRC frame, nearly every SRC image should be usable for calibrated photoclinometry, provided the surface albedo is uniform in the area imaged. This opportunity is also being exploited by Dorrer et al. (2004).

4. MARS EXPLORATION ROVERS ATHENA

4.1 Source Data

The Mars Exploration Rover Spirit landed in Gusev crater on January 4 (UTC), 2004. It was followed 21 days later by the rover Opportunity, which landed on Meridiani Planum. Each rover carries a copy of the Athena science payload (Squyres et al., 2003; Squyres and Athena Science Team, 2004), which includes two science camera systems. The topography, morphology, and mineralogy of the scene around each rover are revealed by the Pancam stereo camera (and also by the

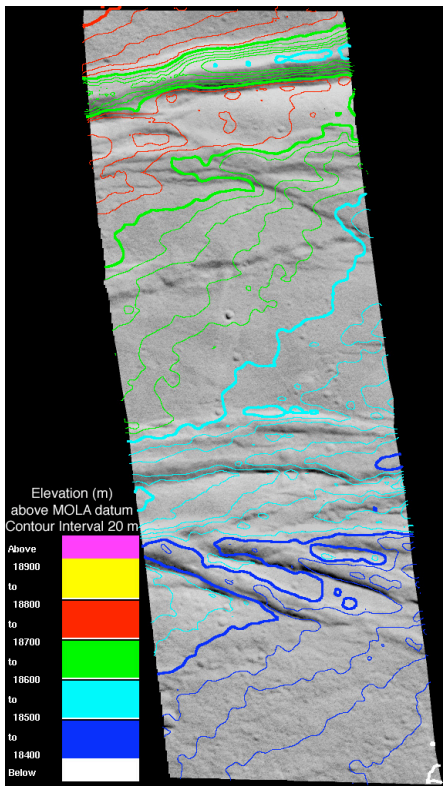

Figure 4. Elevation contours (20 m interval with index contours every 100 m) derived from a DEM compiled from the stereopair shown in Fig. 3 are overlaid on an orthomosaic of the three HRSC-SRC frames. Simple Cylindrical projection, north at top, ground sample distance 15 m for DEM, 4 m for orthomosaic.

Mini-TES thermal emission spectrometer) from 1.5 m above the ground on a mast with azimuth-elevation articulation. Filters on Pancam provide 14 color spectral bandpasses over the spectral region from 0.4 to 1.1 mm. The angular resolution and field of view of the camera are 0.28 mrad/pixel and 16° (Bell et al., 2003). The instrument arm on each rover carries a Microscopic Imager (MI) that is used to obtain high-resolution images of the same materials for which compositional data are obtained. Its spatial resolution is 30 mm/pixel over a 6-mm depth of field (Herkenhoff et al., 2003). The MI has a limited two-band color imaging capability by taking exposures with its yellow-tinted dust cover open and closed. These science cameras are supplemented by several non-color engineering cameras (Maki et al., 2003). Navcam, a stereo camera on the Pancam mast, has a 0.82 mrad/pixel angular resolution and 45° field of view. Pairs of hazard avoidance cameras (Hazcams) with 124° field of view are mounted at the front and rear of the rover.

4.2 Processing Objectives

The USGS has the primary responsibility within the Athena team for processing of the MI images. This processing includes deriving radiometric and geometric calibrations and applying them to all images, creating color images by combining either MI dust cover open/closed image pairs or MI images and overlapping Pancam color image sets, and making MI image mosaics and DEMs derived from MI stereopairs. Additional DEMs and "focal section merges" are produced by Athena team members at JPL and the NASA Ames Research Center by a process of identifying and combining the in-focus sections of images taken at different distances from the target being images. The majority of these objectives could be achieved by a simple processing approach that considers only the MI and ignores constraints on its motion. Because the instrument arm on which the MI rides has only 5 angular degrees of freedom, the position and pointing of the camera are not fully independent, but the

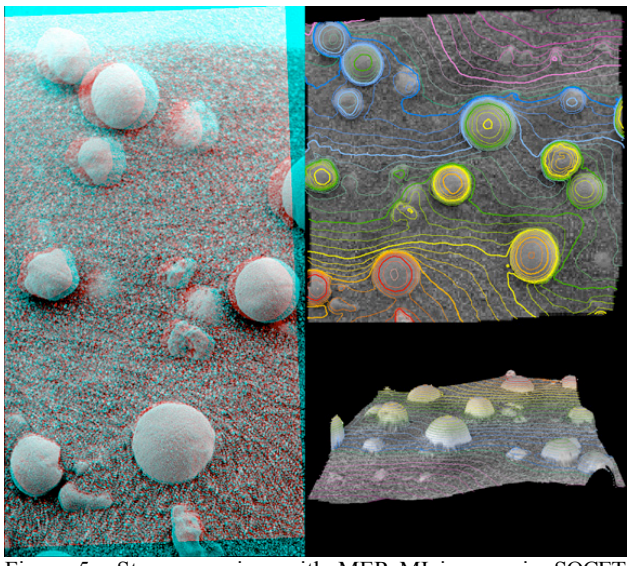

Figure 5. Stereomapping with MER MI images in SOCET SET based on relative orientation without a priori information. Left, anaglyph from two overlapping MI frames obtained by MER-B (Opportunity) rover in Meridiani Planum. Region shown is ~3 cm high. Spherules (informally known as "blueberries") are hematite-rich concretions a few mm in diameter. A third MI frame (not shown) provided stereo coverage overlapping this pair to the right. Upper right: Orthomosaic with contours of "elevation" (in camera-aligned local coordinate system, hence essentially range) derived from the two overlapping stereopairs. CI 250 μm with 1000 μm index contours; range precision is 30 μm. Lower right: perspective view from top, no exaggeration.

constraint is quite weak. As a preliminary approach to our analysis, we demonstrated that a relative orientation of a MI stereopair can be performed in SOCET SET without a priori orientation information (except that the two camera stations were at the best-focus distance from the target, with roughly similar pointing) or constraints. Figure 5 illustrates a microscopic DEM obtained in this way. In order to merge MI images with Pancam color data, however, it is necessary to model the constrained motions of multiple cameras in a consistent coordinate system.

4.3 Methodology

We are meeting the requirement to merge MI and Pancam images by implementing a very general processing software design that includes models of all the MER cameras (except the Hazcams, which could easily be added), their constrained motions, and a large number of related coordinate frames needed to describe these motions. Processing is generally divided into "2D" steps performed in ISIS and "3D" steps done in SOCET SET, as described in Section 3, and in detail resembles the approach developed for the Pancam-like Imager for Mars Pathfinder (Gaddis et al., 1999; Kirk et al., 1999). This includes the implementation of a series of projections relevant to lander/rover data as opposed to global cartography, such as panoramic, planimetric, and oblique orthographic. Bundle-adjustment software must be implemented in ISIS because the SOCET SET adjustment module cannot incorporate the needed constraints. Finally, the SOCET SET stereomatching software is not designed to handle images at multiple azimuths and high elevations relative to the coordinate grid. ISIS must therefore be used to supply SOCET SET with the orientation of each stereopair in a "local" coordinate frame with its Z axis roughly parallel to the camera boresights. DEMs and orthoimages can be produced in this system and transformed back to a "global" coordinate frame in the process of exporting them back to ISIS for further processing.

The Mars Pathfinder mission had only one camera system on a fixed lander, and hence had one "local" coordinate frame

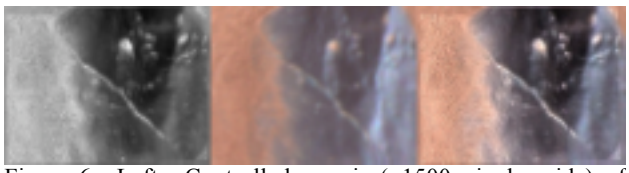

Figure 6. Left: Controlled mosaic (~1500 pixels wide) of two MER-A MI frames showing 4.5-cm area of rock "Mazatzal" partly cleared of dust by brushing with Rock Abrasion Tool. Center: Quasi-natural color Pancam image of same area, resolution ~0.5 mm/pixel. Right: MI and Pancam images merged show correlation of color, texture.

(fixed in the camera head) and one key "global" frame (fixed in the lander and oriented to the vertical and north). Processing software for Pathfinder (including bundle adjustment) was therefore implemented by hard-coding the single type of local-global transformation. For MER, this software had to be generalized to handle coordinates local to several cameras, intermediate coordinates used to model the motion of the Pancam mast and instrument arm, and "global" coordinate frames both moving with the rover and fixed at the initial landing point or subsequent sites of exploration. Fortunately, a powerful mechanism for computing the transformations between the many coordinate frames has been provided by the NASA Navigation Ancillary Information Facility (NAIF; http://pds-naif.jpl.nasa.gov). NAIF supplies Frames Kernels (or F-Kernels) that define the relations between all coordinate frames used by MER (and other missions) in terms of C-Kernels and SP-Kernels that contain the rotations and translations, respectively, between frames. The C- and SP-Kernels can be time-dependent and are continuously updated as the mission proceeds. Routines in the NAIF software library can then be used to obtain the transformation linking any frame to any other at any time.

By using the NAIF kernels and library routines, we are able to compute the a priori orientation of any MER camera in any frame of interest, which allows us to transfer images into SOCET SET, perform unconstrained bundle adjustments there, make DEMs and orthomosaics, and transform these back into ISIS. This capability suffices to make MI products and merge them with Pancam data (Figure 6). We are currently working to extend the NAIF software to compute the partial derivatives of the frame transformations, and to implement a bundle-adjustment program based on the modified frames software. This adjustment program will permit us to make controlled panoramic and planimetric mosaics of Pancam and Navcam images, and to reconstruct the paths of the rovers by linking images obtained from successive stops (cf. Li et al., 2004; Xu, 2004).

ACKNOWLEDGEMENTS

We thank the many individuals at the USGS, Flagstaff who contributed to the work reported: J. Anderson, B. Archinal, J. Barrett, K. Becker, D. Cook, G. Cushing, E. Eliason, L. Gaddis, D. Galuszka, T. Hare, E. Howington-Kraus, C. Isbell, J. Johnson, B. Redding, M. Rosiek, L. Soderblom, R. Sucharski, T. Sucharski, T. Titus, and J. Torson. The work was supported by the following NASA programs: Mars Data Analysis, Mars Express Mission, and Mars Exploration Rovers Mission.

REFERENCES

Albertz, J., et al., 1992. The camera experiments HRSC and WAOSS on the Mars 94 mission. *Int. Arch. Photogramm. Remote Sens*., 29(B1), pp. 130–137.

Archinal, B.A., et al., 2004. Preparing for THEMIS controlled global Mars mosaics. *Lunar Planet. Scil*, XXXV, Abstract # 1903, Lunar and Planetary Institute, Houston (CD-ROM).

Bell, J.F., III, et al., 2003. Mars Exploration Rover Athena Panoramic Camera (Pancam) investigation. *J. Geophys. Res*., 108(E12), 8063, doi: 10.1029/2003JE002070.

Christensen, P., et al. 2003. Morphology and Composition of the Surface of Mars: Mars Odyssey THEMIS Results. *Science*, 300, pp. 2056–2061.

Dorrer, E., et al., 2004. De- and re-shading of Mars Express HRSC image data for homogenization of map relief shading. *Int. Arch. Photogramm. Remote Sens*. (this volume).

Ebner, H., et al., 2004. Improving the exterior orientation of HRSC imagery from Mars-simulations and real data. *Int. Arch. Photogramm. Remote Sens*. (this volume).

Elachi, C. 1987, Introduction to the Physics and Techniques of Remote Sensing, Wiley, pp. 114–141.

Eliason, E., 1997. Production of digital image models using the ISIS system. *Lunar Planet. Sci.*, XXVIII, pp. 331–332, Lunar and Planetary Institute, Houston.

Gaddis, L.R., et al., 1997. An overview of the Integrated Software for Imaging Spectrometers (ISIS). *Lunar Planet. Sci*., XXVIII, pp. 387–388, Lunar and Planetary Institute, Houston.

Gaddis, L.R., et al., 1999. Digital mapping of the Mars Pathfinder landing site: Design, acquisition, and derivation of a cartographic product for science applications. *J. Geophys. Res*., 104(E4), pp. 8853–8868.

Hauber, E., et al., 2004. Planning and preliminary mapping results of the High Resolution Stereo Camera on the ESA Mars Express mission. *Int. Arch. Photogramm. Remote Sens*. (this volume).

Heipke, C., et al., 2004. Performance of automatic tie point extraction using HRSC imagery of the Mars Express mission. *Int. Arch. Photogramm. Remote Sens*. (this volume).

Herkenhoff, K.E., et al., 2003. Athena Microscopic Imager investigation. *J. Geophys. Res*., 108(E12), 8065, doi: 10.1029/2003JE002076.

Jakosky, B. and Mellon, M. 2001. High-resolution thermal inertia mapping of Mars: Sites of exobiological interest. *J. Geophys. Res*., 106(E10), pp. 23887–23908.

Kieffer, H.H., et al. 1977. Thermal and albedo mapping of Mars during the Viking primary mission. *J. Geophys. Res*, 82, pp. 4249–4291.

Kirk, R.L., 1987. Part III. A fast finite-element algorithm for two-dimensional photoclinometry. Ph.D. Thesis (unpubl.), Caltech, pp. 165–258, 1987.

Kirk, R.L., E. Howington-Kraus, and M. Rosiek, 2000a. Recent planetary topographic mapping at the USGS, Flagstaff: Moon, Mars, Venus, and beyond. *Int. Arch. Photogramm. Remote Sens*., XXXIII(B4), 476 (CD-ROM),

Kirk., R.L., et al., 1999. Digital photogrammetric analysis of the IMP camera images: Mapping the Mars Pathfinder landing site in three dimensions. *J. Geophys. Res*., 104(E4), pp. 8869–8887.

Kirk, R.L., et al., 2003a. High resolution toppomapping of candidate MER landing sites with Mars Orbiter Camera narrow-angle images. *J. Geophys. Res*., 108(E12), 8088, doi: 10.1029/2003JE002131.

Kirk, R.L., J.M. Barrett, and L.A. Soderblom, 2003b. Photoclinometry made simple…? ISPRS-ET Working Group IV/9 Workshop "Advances in Planetary Mapping 2003", http://astrogeology.usgs.gov/Projects/ISPRS/MEETINGS/Houston2003/abstracts/Kirk_isprs_mar03.pdf.

Kirk, R.L., K.T. Thompson, and E.M. Lee, 2001. Photometry of the martian atmosphere: An improved practical model for cartography and photoclinometry, *Lunar Planet. Sci.,* XXXII, Abstract #1874, Lunar and Planetary Institute, Houston (CD-ROM).

Kirk, R.L., K.T. Thompson, T.L. Becker, and E.M. Lee, 2000b. Photometric modeling for planetary cartography. *Lunar Planet. Sci*., XXXI, Abstract #2025, Lunar and Planetary Institute, Houston (CD-ROM).

Li., R., K. Di, F. Xu, and J. Wang, 2004. Landing site mapping and rover localization for the 2003 Mars Exploration Rover Mission: Technology and experimental results. *Int. Arch. Photogramm. Remote Sens*. (this volume).

Maki, J.N., et al., 2003. Mars Exploration Rover Engineering Cameras. *J. Geophys. Res*., 108(E12), 8071, doi: 10.1029/2003JE002077.

Malin, M.C., and K.S. Edgett, 2001. Mars Global Surveyor Mars Orbiter Camera: Interplanetary cruise through primary mission, *J. Geophys. Res*., 106(E10), pp. 23,429–23,570.

Mellon, M., et al. 2000. High-Resolution Thermal Inertia Mapping from the Mars Global Surveyor Thermal Emission Spectrometer. *Icarus*, 148, pp. 437–455.

Miller, S.B. and A.S. Walker, 1993. Further developments of Leica digital photogrammetric systems by Helava. *ACSM/ASPRS Annual Convention and Exposition Technical Papers*, 3, pp. 256–263.

Miller, S.B. and A.S. Walker, 1995. Die Entwicklung der digitalen photogrammetrischen Systeme von Leica und Helava. *Z. Photogramm. Fernerkundung*, 1(95), pp. 4–16.

Neumann, G.A., D.D. Rowlands, F.G. Lemoine, D.E. Smith, and M.T. Zuber, 2001. The crossover analysis of Mars Orbiter Laser Altimeter data. *J. Geophys. Res*., 106(E10) pp. 23,753–23,768.

Neukum, G., et al., 2004. The High Resolution Stereo Camera (HRSC) experiment on the ESA Mars Express Mission. *Int. Arch. Photogramm. Remote Sens*. (this volume).

Oberst, et al., 2004. The photogrammetric performance of HRSC in Mars orbit. *Int. Arch. Photogramm. Remote Sens*. (this volume).

Smith, D.E., et al., 2001. Mars Orbiter Laser Altimeter: Experiment summary after the first year of global mapping of Mars. *J. Geophys. Res*., 106(E10), pp. 23,689–23,722.

Squyres, S.W., and the Athena Science Team, 2004. The Athena Mars Rover Science Investigation. *Int. Arch. Photogramm. Remote Sens*. (this volume).

Squyres, S.W., et al., 2003. Athena Mars rover science investigation. *J. Geophys. Res*., 108(E12), 8062, doi: 10.1029/2003JE002121.

Torson, J. and K. Becker, 1997. ISIS: A software architecture for processing planetary images. Lunar Planet. Sci., XXVIII, pp. 1443-1444, Lunar and Planetary Institute, Houston.

Xu, F., 2004. Automation in Mars landing site mapping and rover localization. *Int. Arch. Photogramm. Remote Sens*. (this volume).